

Structure, Mechanical Properties, and Gas Permeability of Elastomers Based on Polybutadiene and Epoxy Resin

Xiaomo Zhang, Shi Ji, Yiwu Quan, Qingmin Chen, Pengshan Chang

Department of Polymer Science and Engineering, School of Chemistry and Chemical Engineering, Nanjing University, Nanjing 210093, China

Received 7 June 2009; accepted 8 January 2010

DOI 10.1002/app.32075

Published online 13 April 2010 in Wiley InterScience (www.interscience.wiley.com).

ABSTRACT: In this study, the structure, gas permeability, and mechanical properties of new elastomers based on liquid polybutadiene and epoxy resin were investigated by dynamic mechanical thermal analysis, thermogravimetric analysis, stress-strain analysis, and water-resistance and gas permeability tests. The results reveal that there was complete phase separation between the epoxy resin and polybutadiene. With increasing epoxy resin content, the glass-transition temperature of the soft segment varied little. These elastomers had tensile strengths of 6–10 MPa

and ultimate elongations of 500–100% according to the different epoxy resin contents. Thermogravimetric analysis revealed that these elastomers had better thermal stability, with a 5% weight loss at a temperature of around 350°C. The gas permeabilities of these elastomers were measured to be 13.2–15.3 barrers for oxygen, 4.8–5.3 barrers for nitrogen, and 28–35 barrers for carbon dioxide at 23°C. © 2010 Wiley Periodicals, Inc. *J Appl Polym Sci* 117: 2366–2372, 2010

Key words: elastomers; polybutadiene; resins

INTRODUCTION

In recent decades, elastomers prepared from the reactive liquid polybutadiene have attracted much attention because of their advantages of low moisture permeability, low glass-transition temperature, and excellent resistance to aqueous acid and bases. Most of these are polyurethanes prepared from hydroxyl-terminated polybutadiene (HTPB), which has been widely used in solid rock propellants, adhesives, and electrical potting compounds. The complete hydrocarbon nature of polybutadiene results in no possibility of hydrogen bonding between the hard and soft segments; this favors phase segregation. There have been many publications on HTPB-based polyurethanes that have dealt with the structure and properties, including the morphology, thermal transition behavior, crosslinking density, mechanical properties, thermal stability, and gas permeability, of these compounds.^{1–10} However, the application of HTPB-based polyurethane has often been hampered by the sensitivity of isocyanate with moisture or water.

On the other hand, epoxy resins are also widely used in many applications, which include coatings, sealants, adhesives, and high-performance composite

materials. The purpose of this study was to explore new elastomers that combine the advantages of polybutadiene and epoxy resin and that may find some applications in place of polybutadiene-based polyurethanes. According to the literature, functionalized liquid polybutadiene has often been used as a toughening agent for the epoxy matrix. The functional group could be an epoxy,^{11–16} carboxyl,^{17–19} or aniline group.²⁰ However, there has been little research reporting elastomers based on polybutadiene and epoxy resin. We discuss the mechanical properties and structure of these new elastomers and evaluate these new polybutadiene networks with respect to their thermal properties, water resistance, and gas permeability.

EXPERIMENTAL

Materials

The epoxy resin (E51), a low-molecular-weight liquid diglycidyl ether of bisphenol A with an epoxide number of 0.51, was supplied by Wuxi Lanxing Co., Ltd. (China). The amine-terminated polybutadiene (ATPB) was Hypro copolymer 2000 × 173 ATB from BF Goodrich Hycar Chemical Group (Akron, OH, USA) with an amine equivalent weight of 900 (an amine value of 62). Triethylenetetramine (TETA) and *m*-xylylenediamine (MXDA) were commercial products and were used as received.

Correspondence to: Y. Quan (quanyiwu@nju.edu.cn).

TABLE I
Formulations of the ATPB-Based Elastomers

Specimen	ATPB (amine function)	TETA (amine function)	MXDA (amine function)	Epoxy resin (epoxy function)	Hard segment (%) ^a
ATP-1	10 g (11 mmol)	0	0	2 g (10.4 mmol)	17
ATP-2	10 g (11 mmol)	0.2 g (9 mmol)	0	4 g (20.8 mmol)	30
ATP-3	10 g (11 mmol)	0	0.4 g (10 mmol)	4 g (20.8 mmol)	30

^a Here *hard segment* is defined as the units including the epoxy resin, TETA, and MXDA (like that of the isocyanate and chain extender in polyurethane).

Preparation of the specimens

The ATPB-based elastomers prepared from ATPB and the epoxy resin E51 were synthesized by the mixture of the materials in different ratios. The weight formulations are outlined in Table I. With and without a combination of other low-molecular-weight amines, ATPB and epoxy resin were completely mixed by a mechanical stirrer and degassed by a Siemens DAC 150FV high-speed mixer (Produced by Hauschild, Herrliberg, Germany) at 3000 rpm. Then, the bubble-free mixtures were poured onto a nylon film with a mold of polytetrafluoroethylene and kept at 50°C for 2 days. The specimens for the tensile strength measurement were 2.0 ± 0.2 mm in thickness.

HTPB-based polyurethane as a control for water-absorption and water-resistance tests was prepared according to the literature.²¹

Measurement and characterization

According to the principles of ASTM D 412-98a, the tensile strength and ultimate elongation were tested with an Instron 4466 instrument (Produced by Instron Co., Norwood, MA, USA) on dumbbell-shaped specimens. The specimens were tested at 23°C at a crosshead speed of 50 mm/min. Each result was obtained by test repetition with three specimens. A Frank hardness tester with a Shore A durometer (Produced by Shanghai Microcre Light-Machine Tech Co., China) was used to measure the hardness of the specimens according to the ASTM D 2240-81 procedure. Cyclic stress-strain behavior measurement was also performed on the Instron 4466 instrument at 23°C. All measurements were performed in a displaced control at a crosshead rate of 10 mm/min. When it reached a certain stress, the specimen was

relaxed at the same crosshead rate until the stress reverted to 0 MPa.

All dynamic mechanical thermal analysis (DMTA) measurements were carried out with a DMA+450 (Metravi B) instrument (tension mode) (Produced by 01 dB- Metravib Co., Lyon, France). The dimensions of the specimens were $20 \times 18 \times 1$ mm³. The frequency was fixed at 1 Hz. The specimens were heated at a nominal rate of 3°C/min from -90 to 150°C. The thermogravimetric analysis (TGA) data were achieved on an Yris 1 thermogravimetric analyzer (PerkinElmer) in an Al₂O₃ crucible in nitrogen at a heating rate of 20°C/min.

For water- and xylene-absorption tests, the films were cut to dimensions of $20 \times 20 \times 2$ mm³, and we determined the dry weight (W_d) and then immersed them in water or xylene at room temperature. We determined the wet weight (W_t) by wiping off the surface water or xylene with paper. The absorbed water or xylene content was then calculated by the following equation:

Absorbed water or xylene content

$$= (W_t - W_d) \times 100 / W_d$$

In the water resistant test, the specimens for stress-strain analysis were immersed in water at

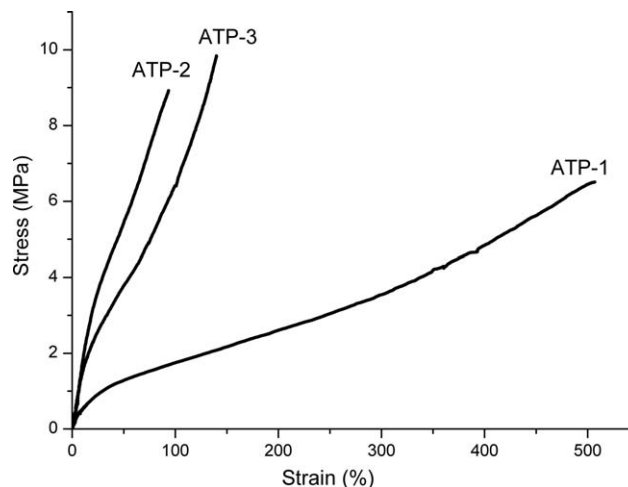


Figure 1 Stress-strain behavior of the ATPB-based elastomers.

TABLE II
Mechanical Properties of the ATPB-Based Elastomers

Specimen	Tensile strength (MPa)	Ultimate elongation (%)	Shore A hardness
ATP-1	6.5	505	65
ATP-2	8.9	90	80
ATP-3	9.8	140	84

TABLE III
Effect of the Thermal History on the Mechanical Properties of the ATPB-Based Elastomers

Specimen	Annealed at 100°C for 1 h		Annealed at 100°C for 2 h	
	Tensile strength (MPa)	Ultimate elongation (%)	Tensile strength (MPa)	Ultimate elongation (%)
ATP-1	6.6	480	6.9	510
ATP-2	8.8	92	8.6	85
ATP-3	9.6	135	10.2	150

50°C. The tensile strength was tested after different immersion times.

The apparatus and experimental procedure for gas permeability testing were described by Chen.²² The gas permeability was determined as follows:²³

$$\text{Permeability} = q/(\Delta P \times L \times A)$$

where q is the volumetric flow rate of gas permeation [cm^3 (STP)/s], L is the membrane thickness (cm), ΔP is the pressure difference across the membrane (cmHg), and A is the effective membrane area (cm^2). The gas permeability is expressed in barrers [10^{-10}cm^3 (STP)/ $\text{cm}^3 \text{s cmHg}$].

RESULTS AND DISCUSSION

Mechanical properties

The weight formulations and mechanical properties of ATPB-based elastomers are listed in Tables I and II. As for the ATP-2 and ATP-3 specimens, TETA and MXDA were selected hardeners to cure the epoxy resin in the formulation (the total epoxy groups per total amine functions are calculated in Table I). The stress–strain behavior of these elastomers was investigated (shown in Fig. 1). As shown in Figure 1 and

Table II, it was clear that the tensile strength of these materials changed profoundly when the hard-segment content increased from 17 to 30 wt %. The tensile strengths of ATP-2 and ATP-3 reached to 9–10 MPa. However, the ultimate elongation decreased dramatically with increasing hard-segment content. In agreement with later dynamic mechanical studies, the stress–strain behavior of these ATPB-based elastomers was nearly unaffected by the thermal treatment. Here, the specimens ATP-1, ATP-2, and ATP-3 were annealed at 100°C for as long as 1 or 2 h followed by air quenching. The results of the stress–strain analysis are outlined in Table III. The mechanical properties of these elastomers were shown to be highly time-independent because of high phase separation, such as with HTPB-based polyurethane.⁴

Cyclic stress–strain behavior measurement was also performed on the Instron 4466 instrument at 23°C. When it reached a certain stress, the specimen was relaxed at the same crosshead rate until the stress reverted to 0 MPa. We continuously tested the specimens for four tension/unloading cycles in total, and the results are included in Figures 2–4 (insert: the remnant strain after each cyclic tension/unloading). It was clear that an irreversible tension/unloading behavior was observed, and a partial hysteresis

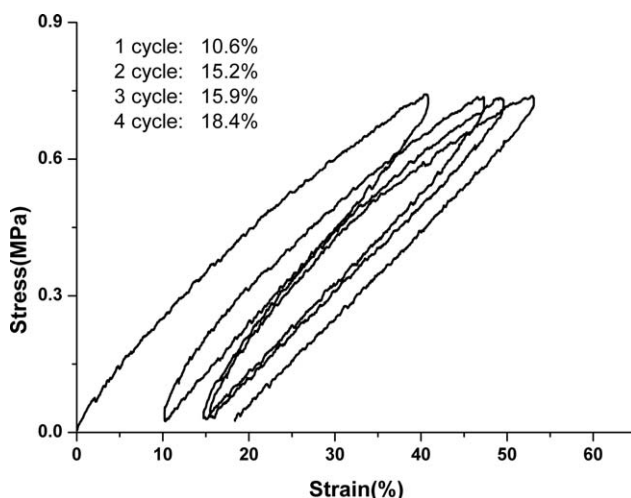


Figure 2 Cyclic stress–strain behavior during tension of specimen ATP-1 (four times in all). The insert shows the remnant strain after each tension/unloading cycle.

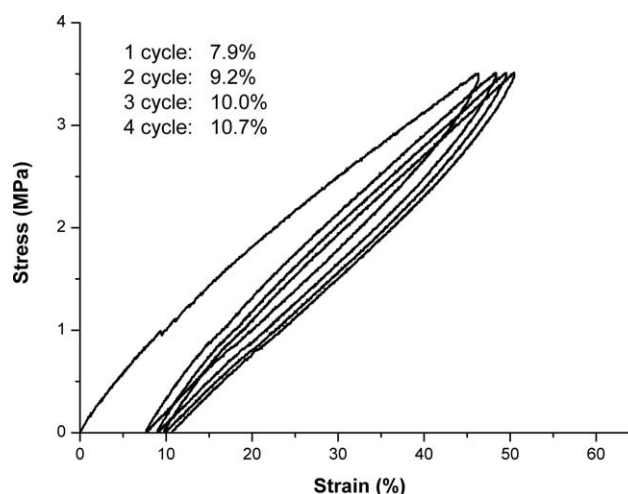


Figure 3 Cyclic stress–strain behavior during tension of specimen ATP-2 (four times in all). The insert shows the remnant strain after each tension/unloading cycle.

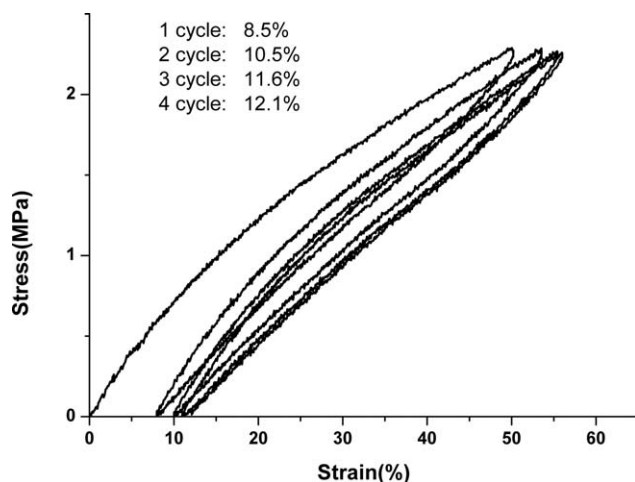


Figure 4 Cyclic stress-strain behavior during tension of specimen ATP-3 (four times in all). The insert shows the remnant strain after each tension/unloading cycle.

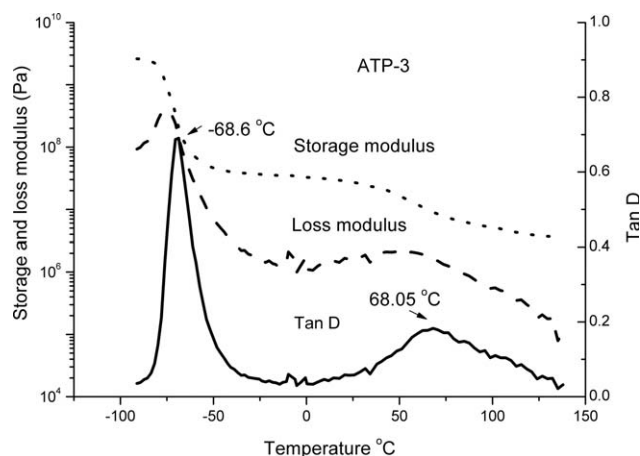


Figure 7 DMTA for specimen ATP-3.

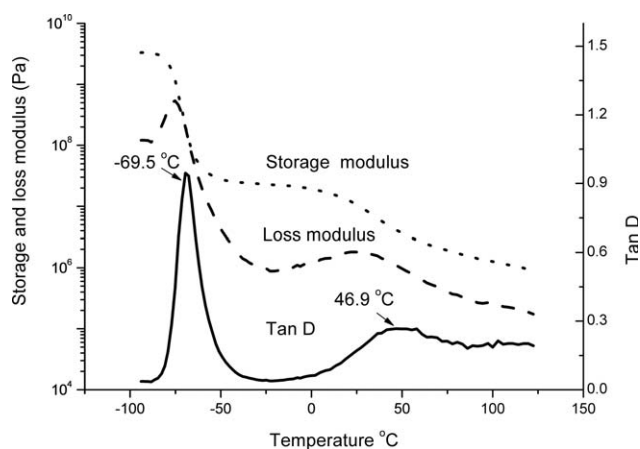


Figure 5 DMTA for specimen ATP-1.

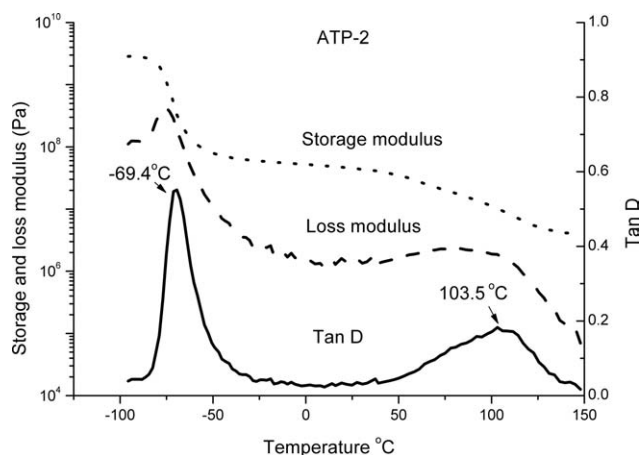


Figure 6 DMTA for specimen ATP-2.

curve was obtained, as shown in Figures 2–4. Remnant strains of 10.6, 7.9, and 8.5% were observed after the first unloading for specimens ATP-1, ATP-2, and ATP-3, respectively. After subsequent cyclic compression/unloading, there was a small increase in the later remnant strain for three specimens. This stress-softening behavior is characteristic of phase-separated materials.⁴ Moreover, the higher the hard-segment content was, the lower the remnant strain was, presumably because of higher crosslinks in ATP-2 and ATP-3 with the addition of TETA or MXDA.

DMTA

Figures 5–7 show the DMTA results for the specimens ATP-1, ATP-2, and ATP-3, respectively, and a comparison of the temperature dependence of the loss tangent ($\tan \delta$) is shown in Figure 8. From Figure 8, we concluded that the glass-transition temperature of the soft segment appeared at -68 to -70°C .

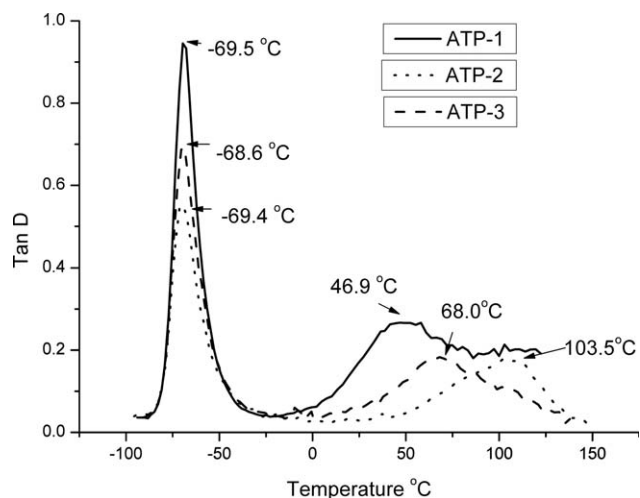


Figure 8 Temperature dependence of $\tan \delta$ of the ATPB-based elastomers.

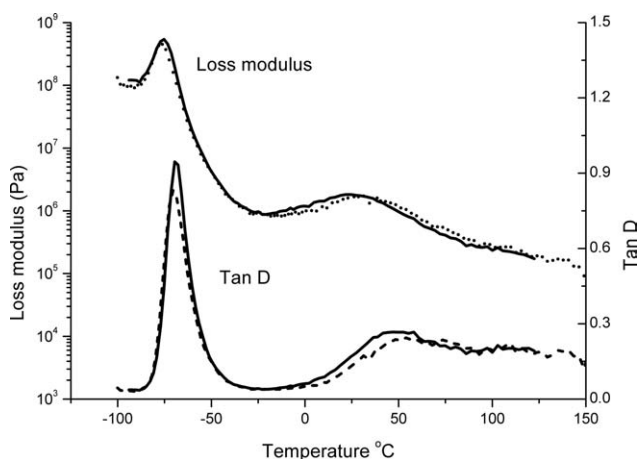


Figure 9 Dynamic mechanical response of ATP-1: (—) quenched from 100°C and retested immediately and (---) quenched from 100°C and retested after 1 month.

The value of the glass-transition temperature in these elastomers was compared to a value of -70°C for HTPB-based polyurethane,²¹ and its invariance with increasing epoxy resin content indicated that phase segregation was very nearly complete. Because amine and epoxy groups form amorphous hard regions, the driving force for phase segregation must have come from the extreme incompatibility of the polar hard segment and the apolar soft segment. The higher temperature broad peak of $\tan \delta$ could have been directly attributed to hard segments with different length, which dispersed in the soft segment.

Like the behavior of HTPB-based polyurethane,⁴ the dynamic mechanical properties of the ATPB-based elastomers were also almost unaffected by the thermal history (shown in Fig. 9). One specimen was quenched to a liquid nitrogen temperature from 100°C and immediately tested, and the other was

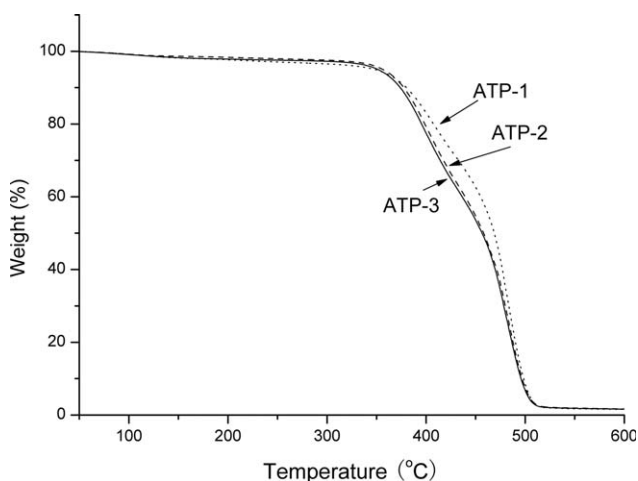


Figure 10 TGA curves of the ATPB-based elastomers.

TABLE IV
Weight-Loss Data of the ATPB-Based Elastomers

Specimen	ATP-1	ATP-2	ATP-3
Temperature at 5% weight loss ($^{\circ}\text{C}$)	348	351	356
Temperature at 10% weight loss ($^{\circ}\text{C}$)	380	373	377
Temperature at 20% weight loss ($^{\circ}\text{C}$)	407	395	398

annealed at 100°C for as long as 2 h, which was followed by air quenching for 30 days. DMTA testing showed that the glass-transition temperature of the soft segment was essentially unchanged.

Thermal stability

The thermal studies were carried out by TGA. Figure 10 indicates the thermal degradation of the ATPB-based elastomers, and Table IV shows the decomposition temperature at various weight loss percentages. As shown in Figure 10, a three-step degradation was observed in all of the thermogravimetric curves of the three ATPB-based elastomers. The elastomers were stable up to 340°C and remained almost intact in the first step. The quantity of gaseous components, mainly water and trapped solvent, released in this step was relatively small. In the first step, the weight loss was less than 3%. The decomposition of step 2 corresponded to the amine-epoxy bond breaking, and step 3 was the polybutadiene decomposition. Almost complete decomposition was observed at about 500°C.

Generally, HTPB-based polyurethane elastomers have a 5% weight loss before 300°C, usually around 280°C, and the rapid weight loss starts at approximately 300°C and continued up to 350°C, which corresponded to the urethane bond breaking.^{24,25} For the elastomers based on polybutadiene and epoxy resin, as shown in Table IV, they exhibited a much

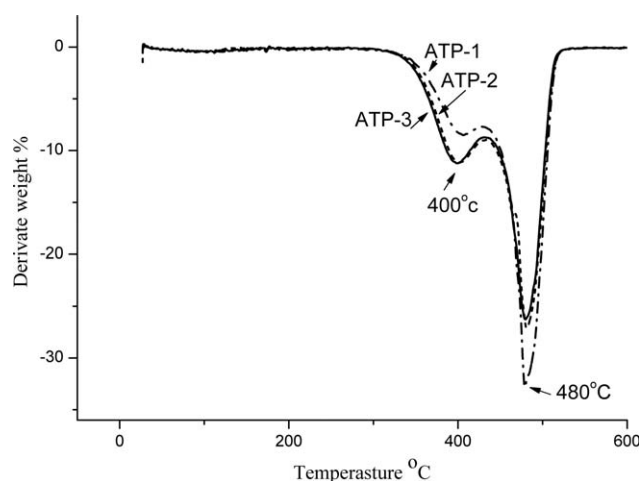


Figure 11 Derivative weight curves in TGA for the ATPB-based elastomers.

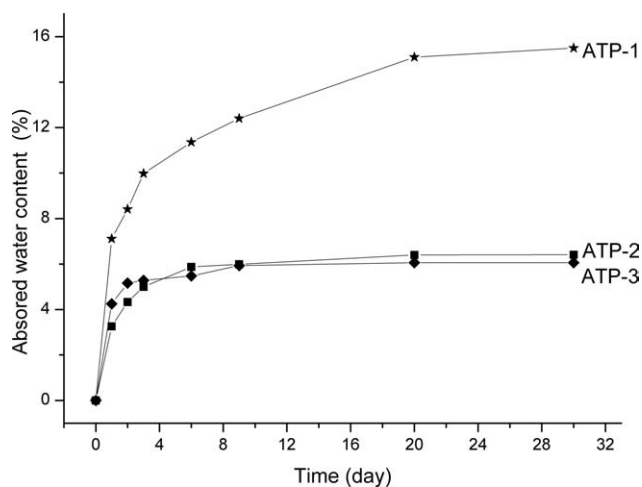


Figure 12 Water absorption of the ATPB-based elastomers.

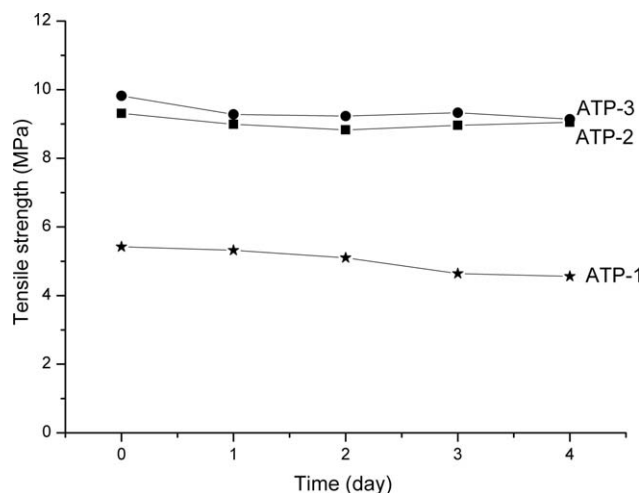


Figure 13 Effect of water on the tensile strength of the ATPB-based elastomers at an elevated temperature (50°C).

better thermal stability with a 5% weight loss at a temperature of around 350°C.

Figure 11 shows the derivative weight curves in TGA for the ATPB-based elastomers. It was more clear that there were two main peaks in the temperature ranges of 350–430 and 430–500°C in all curves. These two peaks corresponded to the second- and third-stage decomposition of the elastomers, as shown in the TGA curves. In the second step of degradation, the higher hard-segment content in specimens ATP-2 and ATP-3 resulted in a bigger exothermic peak, which validated that conclusion that the decomposition of the amine–epoxy bond occurred between 350 and 430°C, and step 3 was the polybutadiene decomposition.

Water/xylene-absorption and water-resistance tests

Figure 12 shows curves of the percentage increase in mass after the sample was immersed in water at room temperature. After it was immersed in water for 30 days, the specimen ATP-1 absorbed about 15 wt % water. With the increase in hard segment, there was a significant decrease in water absorption. For example, the specimens ATP-2 and ATP-3 only absorbed 6 wt % water after they were immersed in water for 30 days. To explain the high water absorp-

tion of ATP-1, swelling tests were performed on $20 \times 20 \times 2 \text{ mm}^3$ specimens by the immersion method in xylene at 23°C. The equilibrium of solvent absorption was established in 72 h; with more immersion time, the weight did not increase any more for any of the specimens. The swelling percentages of the elastomers after 72 h were 376, 128, and 146% for ATP-1, ATP-2, and ATP-3, respectively. After they were extracted by xylene, the samples had gel fractions of 86% for ATP-1, 96.8% for ATP-2, and 95.6% for ATP-3. From these data, we concluded that the swelling percentage of elastomers varied markedly with increasing hard-segment content. The introduction of TETA or MXDA helped to improve the cross-links in the elastomers, which increased the gel fraction and decreased the swelling percentage and water absorption.

The tensile strengths of the specimens before and after some days of water immersion are shown in Figure 13. After immersion, the specimens were dried again at 60°C for 4 h *in vacuo* to eliminate the absorbed water. It is well known that absorbed water exerts a plasticizing effect in elastomers, which decreases the tensile strength. Tests gave us the relatively exact results of hydrolytic degradation in the ATPB-based elastomers. The results reveal that all of the specimens showed better

TABLE V
Oxygen, Nitrogen, and Carbon Dioxide Permeability of the ATPB-Based Elastomers at 23°C Under 0.1 MPa

Specimen	Hard segment (%)	Oxygen (barrer)	Nitrogen (barrer)	Carbon dioxide (barrer)	O ₂ /N ₂ selectivity
ATP-1	17	15.3	5.2	28.9	2.94
ATP-2	30	13.2	4.3	34.5	3.02
ATP-3	30	14.1	4.8	32.5	2.93

water resistance. After 96 h of immersion in water at 50°C, the mechanical properties of specimen ATP-1 were somewhat reduced, and the sample retained about 84% of its initial value in tensile strength. Meanwhile, specimens ATP-2 and ATP-3 retained 93 and 97%, respectively, of their initial values in tensile strength. The water resistance of HTPB-based polyurethane was also investigated as a control. After 96 h of immersion in water at 50°C, HTPB-based polyurethane also retained more than 95% of its initial value in tensile strength. In general, HTPB-based polyurethane showed somewhat better water resistance than the ATPB-based elastomers.

Gas permeation measurement

The oxygen, nitrogen, and carbon dioxide permeabilities were measured, and the O₂/N₂ selectivity was calculated. As shown in Table V, the gas permeabilities of these elastomers were measured to be 13.2–15.3 barrers for oxygen, 4.8–5.3 barrers for nitrogen, and 28–35 barrers for carbon dioxide at 23°C. The oxygen and nitrogen permeability of the elastomers decreased slightly as the hard-segment content increased from 17 to 30%; this result also implied that most gases passed through the soft-segment-containing region of the membrane. In general, the value of the oxygen permeability of the ATPB-based elastomers was comparable to that of HTPB-based polyurethane.²⁴ However, the O₂/N₂ selectivity was calculated to be around 3.0, which was 10–20% higher than that of HTPB-based polyurethane.²³

CONCLUSIONS

New elastomers were prepared from ATPB and epoxy resin. DMTA and stress–strain analysis indicated that there was complete phase separation in these ATPB-based elastomers, and the structure and mechanical properties of these elastomers were almost unaffected by the thermal history. These elastomers had tensile strengths of 6–10 MPa and ultimate elongations of 500–100%. With the addition of other low-molecular-weight amines, the tensile strength and water resistance of the elastomers increased significantly. The oxygen permeability of

the ATPB-based elastomers was comparable to HTPB-based polyurethane, and the O₂/N₂ selectivity was 10–20% higher than that of HTPB-based polyurethane.

The authors gratefully acknowledge two anonymous reviewers for their constructive comments and helpful suggestions.

References

1. Lagasse, R. R. *J Appl Polym Sci* 1977, 21, 2489.
2. One, K.; Shimada, H.; Nishimuro, T.; Yamashita, S.; Okamoto, H.; Minoura, Y. *J Appl Polym Sci* 1977, 21, 3223.
3. Schneider, N. S.; Matton, R. W. *Polym Eng Sci* 1979, 19, 1122.
4. Brunette, C. M.; Hsu, S. L.; Rossman, M.; MacKnight, W. J.; Schneider, N. S. *Polym Eng Sci* 1981, 21, 668.
5. Kothandaraman, H.; Nasar, A. S. *J Appl Polym Sci* 1993, 50, 1611.
6. Manjari, R.; Somsundaram, U. I.; Joseph, V. C.; Sriram, T. *J Appl Polym Sci* 1993, 48, 279.
7. Huang, S. L.; Lai, J. Y. *Eur Polym J* 1997, 33, 1563.
8. Nair, P. R.; Nair, C. P. R.; Francis, D. J. *J Appl Polym Sci* 1999, 71, 1731.
9. Desai, S.; Thakore, I. M.; Sarawade, B. D. *Eur Polym J* 2000, 36, 711.
10. Yang, J. M.; Lin, H. T. *J Membr Sci* 2001, 187, 159.
11. Bussi, P.; Ishida, H. *Polymer* 1994, 35, 956.
12. Bussi, P.; Ishida, H. *J Appl Polym Sci* 1994, 53, 441.
13. Latha, P. B.; Adhinarayanan, K.; Ramaswamy, R. *Int J Adhes Adhes* 1994, 14, 57.
14. Jaehyung, L.; Gregory, R. Y.; Thein, K. *Polymer* 2005, 46, 12511.
15. Soares, B. G.; Leyva, M. E.; Moreira, V. X.; Barcia, F. L.; Khastgir, D.; Sima, R. A. *J Polym Sci Part B: Polym Phys* 2004, 42, 4053.
16. Barcia, F. L.; Amaral, T. P.; Soares, B. G. *Polymer* 2003, 44, 5811.
17. Nigam, V.; Setua, D. K.; Mathur, G. N. *J Appl Polym Sci* 1998, 70, 537.
18. Dusek, K.; Lednický, F.; Lunak, S.; Mach, M.; Duskova, D. In *Rubber-Modified Thermoset Resins*; Riew, C. K.; Gillham, J. K., Eds.; ACS Advances in Chemistry Series 208; American Chemical Society: Washington, DC, 1984; p 27.
19. Shukla, S. K.; Srivastava, D. *J Appl Polym Sci* 2006, 100, 1802.
20. Kar, S.; Banthia, A. K. *J Appl Polym Sci* 2005, 96, 2446.
21. Quan, Y. W.; Wang, Q. J.; Dong, W. Z.; Chen, Q. M. *J Appl Polym Sci* 2003, 89, 2672.
22. Chen, S. H.; Lai, J. Y. *J Appl Polym Sci* 1996, 59, 1129.
23. Ruan, R. C.; Ma, W. C.; Chen, S. H.; Lai, J. Y. *J Appl Polym Sci* 2001, 82, 1307.
24. Huang, S. L.; Lai, J. Y. *J Appl Polym Sci* 1995, 58, 1913.
25. Nair, P. D.; Jayabalam, M.; Krishnamurthy, V. N. *J Polym Sci Part A: Polym Chem* 1990, 28, 3775.